NOVEL $K_2W_7O_{22}/Ti_3C_2$ NANO-COMPOSITE BASED SENSOR DEVICE FOR BREATH ACETONE ANALYSIS IN TYPE-1 DIABETES

A Thesis
Submitted to the Graduate Faculty
of the
North Dakota State University
of Agriculture and Applied Science

By

Obinna Henry Ama

In Partial Fulfillment of the Requirements
for the Degree of
MASTER OF SCIENCE

Major Program:
Biomedical Engineering

August 2020

Fargo, North Dakota

North Dakota State University

Graduate School

Title

NOVEL $K_2W_7O_{22}/Ti_3C_2$ NANO-COMPOSITE BASED SENSOR DEVICE FOR BREATH ACETONE ANALYSIS IN TYPE-1 DIABETES

By

Obinna Henry Ama

The Supervisory Committee certifies that this ***disquisition*** complies with North Dakota State University's regulations and meets the accepted standards for the degree of

MASTER OF SCIENCE

SUPERVISORY COMMITTEE:

Dr. Benjamin Braaten

Chair

Dr. Lopez-Martinez Giancarlo

Dr. Kouhyar Tavakolian

Approved:

August 12, 2020

Date

Dr. Annie Tangpong

Department Chair

ABSTRACT

Acetone in exhaled breath is gaining attention as a non-invasive means of quantifying blood glucose levels in Diabetics. This calls for development of novel biosensors for the detection of trace concentrations of acetone present in human breath. Traditional gas detection systems, such as GC/MS and chemiresistive sensors, are currently used for this purpose. However, these systems have limitations with regards to size, cost, and operating temperature. This work presents the $K_2W_7O_{22}/Ti_3C_2$ nanocomposite sensor as breath acetone sensor that overcomes the limitations in traditional detection systems. Sensing experiments were conducted using 5 different sensor materials in varying ratios. KWO/Ti_3C_2 - ratio 2:1 (annealed) and KWO/Ti_3C_2 - ratio 2:1 (Unannealed) showed excellent sensitivity to 2.85ppm and 5.4ppm acetone concentration. These materials were then implemented in a prototype device. Material and device test results confirm the potentials of the novel KWO/Ti_3C_2 nanocomposite as a good sensor for breath acetone detection.

ACKNOWLEDGEMENTS

I wish to express my sincere sentiment of gratitude to the following individuals who made my academic journey at NDSU a success. Firstly, I am grateful to my Supervisors; Dr. Danling Wang and Dr. Benjamin Braaten, for the privilege to join their lab, their support and constant supervision through my studies. This has positively impacted my ability to work independently in any research endeavor. Additionally, I wish to thank Dr. Benjamin Braaten, Dr. Ivan Lima, Dr. Lopez-Martinez, Dr. Qifeng Zhang, Dr. Roger Greene, Dr. Kouhyar Tavakolian and Dr. Kalpana Katti for pointing me in the right direction each time I had questions. I want to say a big thank you to present and former colleagues; Srilakhshmi Gundlakunta, Michael Johnson, Rezuan MD Hossain, Sudipto Saha, Fadilah Altayran and Anna Rudie for their support and assistance during my work.

Lastly, I wish to appreciate my wife – Vivian Ama, my parents and siblings for their constant love, support and motivation through my academic pursuit at North Dakota State University.

DEDICATION

To the loving memory of my Mum.

TABLE OF CONTENTS

LIST OF TABLES

LIST OF FIGURES

INTRODUCTION

The number of people living with diabetes worldwide has continued to increase with nearly 463 million adults between ages 20-79, as reported by the International Diabetes Federation (IDF)(1). Future projections estimate this number to increase to approximately 700 million people by 2045(1). These alarming findings make diabetes a global health emergency that places far reaching impact on mortality rates and economic productivity, if urgent measures are not taken to curb this growing concern.

Diabetes occurs as a result of a compromised regulation of blood glucose level, which largely stems from an impairment in the ability of the pancreas to produce insulin or the body's inability to respond to the insulin – a hormone responsible for regulating the amount of glucose in the blood. The acceptable blood sugar level for normal individuals is reported to be within 800 - 1000ppm range(2), however, elevated blood sugar levels beyond this range (also known as hyperglycemia), have been associated with diabetic subjects(3). There are 3 known types of diabetes; Type-1 (T1D), Type-2 (T2D) and Gestational Diabetes Mellitus (GDM)(1,4). T1D is caused by an auto-immune reaction, where the body's immune system fights the beta cells that produce insulin(5). This reaction accounts for the lack of or low concentration of insulin produced by the pancreas in patients suffering from T1D. The exact causes for this auto-immune response in T1D is not yet known, but there have been links to several genetic and environmental factors(6,7). In T2D, the body manifests a characteristic resistance to insulin; it does not respond to insulin(8). As a result, blood glucose continues to rise unabated. T2D is commonly diagnosed in older adults. GDM on the other hand, consists of high blood sugar levels during pregnancy, a condition which is known to disappear after pregnancy, but predisposes both mother and child to risks of developing T2D later on in life(9).

If not effectively managed, diabetes has been reported to lead to complications ranging from obesity, nerve damage, and sexual problems to increased risk of heart problems. Effective management of diabetes demands frequent monitoring of blood sugar levels, to prevent exacerbation due to unchecked hyperglycemia. Furthermore, quantitative knowledge of blood sugar level is a crucial step in deciding the line of treatment such as meal plans, exercise and insulin dose.

Recently, a variety of blood glucose measurement techniques have been introduced into practice, while some are yet in their conceptual stages. One of such studies currently gaining attention is the study on the concentration of acetone produced in exhaled breath, intended to serve as a potential indicator of blood glucose level(10). Acetone is known to be produced in the body through a process known as ketoacidosis; when the liver breaks down fats to produce energy in response to the body's inability to utilize glucose(11). Consequently, acetone as a byproduct of ketoacidosis in diabetics, is present in several channels of excretion as in exhaled breath(11). On the one hand, since there are other sources of acetone in the body other than ketoacidosis, studies have shown that breath acetone levels for healthy individuals manifest between 0.4ppm to 0.9ppm. While on the other hand, the concentration is about 1.8ppm and above for diabetics. Conversely, individuals with acetone levels between 0.9 and 1.8 are said to be at risk of developing diabetes(11–13).

This work will mainly focus on the quantitative analysis of breath acetone and ensuing results will potentially serve as a prelude to establishing a standard correlation between breath acetone concentration and blood glucose levels, in future studies. For some context in this discourse, a review of past and current methods for quantitative analysis of acetone in exhaled breath, would be appropriate.

Literature Review

Different techniques have been devised to determine the concentration of acetone in exhaled breath. The Gas chromatograph (GC) used in conjunction with a Flame Ion Detector (FID) or Mass Spectrometer (MS)(14–16), has been a standard method for quantification of breath acetone. The combination of these modalities allows for high specificity during detection, but are characterized with a slow response time, bulky and require sample preparation. Real-time detection of breath acetone has also been made possible with the use of proton transfer reaction mass spectrometry (PTR-MS) and the selected ion flow tube mass spectrometry (SIFT-MS)(14). This technique makes it possible to track minute changes in concentration with high resolution and specificity. The PTR-MS and SIFT-MS do not require sample preparation but are also costly, bulky and require frequent calibration(14).

Sensor Material

To address the challenges associated with size, cost and complexity of these traditional analytical techniques for breath acetone, attention started shifting towards the use of electronic nose devices that integrate chemiresistive gas sensors, metal-oxide semiconductor gas sensors and conductive polymer gas sensors(17,18). These materials exceed the limitations of traditional gas sensing systems in terms of cost, portability and simplicity. They work based on fundamental electrochemical principles, which is changing electrical properties in response to changing gas concentration(18). In other words, exposure to target gases, elicit reversible changes in the electrical properties (resistivity) of chemiresistive sensors(18,19). Despite the advantages of size and cost, they need to be designed for high selectivity, in order to favorably compete with the conventional analytical systems that are known to be highly discriminatory in their function. The most studied chemiresistive sensors currently employ metallic oxide semiconductors (MOS) as the

active sensing layers for detecting gases. These MOS active sensing layers include; Tungsten (VI) oxide (WO_3), Tin(IV) Oxide (SnO_2), Zinc oxide (ZnO), Titanium dioxide (TiO_2), Iron (III) oxide(Fe_2O_3), Indium (III) oxide ($In2O_3$), and Copper (II) oxide (CuO)(20). Several reviews have extensively discussed the sensing performance of these materials, either in their pure or hybrid states(17,20–24).

The use of nanomaterials has been considered an attractive element in clinical diagnostics by breath analysis, because of their large specific surface area, porosity, fast reaction, and cost-effective growth technique. Furthermore, the large surface to volume ratio of nanostructured metal oxides (NMOs) is critical to achieve high sensitivity due to the increased gas reaction sites on the surface(18,24,25).

Improved sensing performance of chemiresistive sensors have also been achieved through the combination of active nanostructured MOS sensing layers or/and metal compounds. The resultant hybrid sensing layer achieves an improved sensing performance due to the individual attributes of the elemental materials given the large surface area to volume ratio (SVR), cost effective growth technique, porosity and fast response time. The SVR is very critical to achieving high sensitivity due to an increased number of gas interaction sites on the material surface. An example is the chemiresistive acetone sensor, indium loaded (In/WO_3-SnO_2) which shows good sensitivity, selectivity and fast response time(26), in contrast to the SnO2 sensor. However, excellent sensitivity of the In/WO_3-SnO_2 sensor is a function of its operating temperature (200^oC). In contrast, Potassium Tungsten Oxide - $K_2W_7O_{22}$ (KWO), a novel semiconductor nanomaterial, has recently been fabricated for room temperature detection of acetone(27,28). Experimental results have shown that its sensing mechanism is based on its p-type semiconductor property, high surface area and room temperature ferroelectric property. These features enable its interaction with

the high dipole moments of the acetone molecules, thereby increasing the resistivity of KWO(29). Another nanomaterial of interest in this study is the Ti_3C_2. It belongs to the new class of 2-D materials called Mxene and it is fast gaining attention in the field of biomedical sensing(30). A recent study showed its sensitivity to 100ppm acetone and its superb performance is attributed to its high surface area, high electrical conductivity and functionalized surfaces(31). These properties bestow the MXene sensors with a characteristic high signal to noise ratio (SNR) and high selectivity due to functionalized surface(32–34).

Table 1: Selected MOS active sensing layers for acetone detection.

Material	**Principle of Operation**	**Limit of Detection**	**Response Time**	**Operation Temperature**
In_2O_3 (35)	ΔR	25ppm	~10 s (in N_2)	400 °C
InN(36)	ΔR	0.4 ppm	150 s for 10 ppm (in air)	200 °C
GaN(37)	ΔR	500 ppm	10 s for 1,000 ppm (in air)	350 °C
WO_3 (38)	ΔR	0.2ppm	~3.5 m	400 °C
ZnO + Ni +UV light (39)	ΔR	100ppm	5 min (in air)	Room Temperature
ZnO (40)	ΔR	100ppm	30 s	200 °C
LaFeO3(41)	ΔR	500ppm	33 s (in air)	275 °C
TiO_2 (42)	ΔR	1 ppm	10 s (in air)	500 °C
KWO(28,29)	ΔR	2.85ppm	30s (in air)	Room temperature

Sensor Devices

The emergence of these enhanced MOS sensing materials have opened up new frontiers in the fabrication of current gas sensors with regards to complexity, size, power consumption and overall cost, in direct comparison to traditional devices such as the lab-type GC/MS, FT-IR, etc.

These traditional devices are commercially available from about $20, 000 to $100, 000 and weigh between 15kg to 75kg. Their characteristic high price and non-portability makes them affordable to mostly corporations and research institutions. However, recent advancements in the field of electronics such as advanced integrated circuits, improved fabrication techniques and enhanced data processing techniques has enabled the design of low-cost, micro-sized, and low-power consuming gas sensor devices that are capable of interfacing with smart gadgets like cell phones and tablets. These features make these devices available and applicable in everyday use in the monitoring of diseases such as diabetes. Typically, a gas detection device consists of a gas delivery and detection module, data acquisition board and a computer for data analysis. Nonetheless, a low-cost portable sensing device in focus, will rather comprise of a sensor module, a signal conditioning circuitry and a data visualization and analysis unit.

Two obvious drawbacks for most MOS chemiresistive sensors are the high operating temperature which relies on a heater system and secondly, the high impedance characteristics of these sensors (20MΩ to 150MΩ). This high impedance makes it difficult to obtain repeatable sensing data; particularly due to their tendency to be easily affected by external noise, bias currents, and distant charges which accounts for the characteristic initial resistance baseline shift of many chemiresistive MOS sensors. However, with specific material enhancement (such as use of nanocomposites), improved circuit design and fabrication techniques, these limitations can be addressed.

Problem Statement

Based on these foundations, this work is aimed at addressing the prevailing limitations associated with conventional measurement techniques for breath acetone - by exploring the combined potentials of KWO and Ti_3C_2 as a novel nanocomposite sensor material for low-cost,

highly sensitive room-temperature detection of breath acetone. Both materials were synthesized, and sensitivity experiments conducted to show sensitivity of the novel nanocomposite sensor and thereafter implemented in a prototype device as a proof of concept.

MATERIALS AND METHODS

Material Synthesis

The KWO semiconductor nanomaterial was grown using the hydrothermal method and synthesized as described in a previous report(29). The resultant material was characterized using a Thermo Electron K-Alpha X-ray photoelectron spectroscopy (XPS)(Thermo Fischer Scientific, Waltham, MA, USA) and X-ray diffraction (XRD) was done on a Bruker AXS D8 Discover (Bruker AXS Inc., Madison, WI, USA) to study the as-synthesized KWO crystalline structure(27).

The synthesis of Ti_3C_2 MXene was achieved in two steps as described in(34). The first step involved the fabrication of the MAX phase (Ti_3AlC_2) using TiC, Ti, and Al powders in the required stoichiometric ratio. The second step was to yield the Ti_3C_2 Mxene from the Ti_3AlC_2 MAX phase through an etching process. The aluminum (Al) in the synthesized Ti_3AlC_2 bulk is etched from the bulk using Hydrofluoric acid (HF) at room temperature, leaving behind the Ti_3C_2 nanosheets with numerous interlayer spaces which increases the surface area to volume ratio of the resultant Mxene material(43). XRD and FT-IR data were obtained to confirm the morphology and functionalization of the resultant Ti_3C_2 Mxene.

The nanocomposite film of KWO and Ti_3C_2 was made by mixing the solids into 2 distinct ratios of KWO/Ti_3C_2 - ratio1:2 and KWO/Ti_3C_2 - ratio 2:1. Finally, 5 nanomaterial samples comprising of Ti_3C_2, KWO, KWO/Ti_3C_2 - ratio1:2 (annealed), KWO/Ti_3C_2 - ratio 2:1 (annealed) and KWO/Ti_3C_2 - ratio 2:1 (unannealed) were made into thin films by the drop-cast method on 5 separate gold-electrode patterned glass substrates.

Testing System

For a typical chemiresistive material, the sensitivity of the film when exposed to the analyte gas, correlates with the change in its electrical resistance. In the case of KWO/Ti_3C_2 film, a couple

of factors have previously been reported to significantly impact its sensitivity to acetone. They include the baseline resistance of the film, Relative humidity (RH) conditions and the flowrate of acetone(44). Hence, the testing system as illustrated in Figure 1, was designed to account for the effect of these key parameters.

Acetone (99.5%) was obtained from Sigma Aldrich. The OVG-4 vapor generator by Owlstone Inc. was used to vaporize liquid acetone and control RH during the experiment. The change in resistance across the film was measured using the Keithley electrometer. RH was measured using an RH monitor.

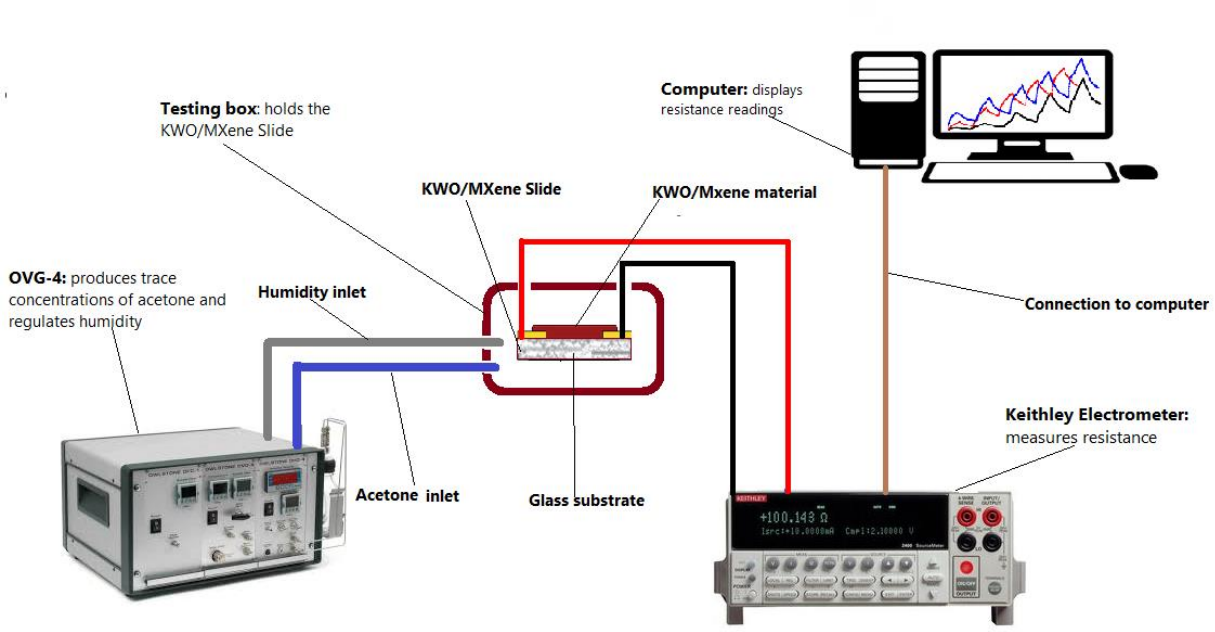

Figure 1: Functional diagram of the acetone testing system. Acetone and humidity are generated by the OVG and delivered into the sensor testing box. The humidity and acetone inlet lines control the flow of RH and acetone respectively.

The vapor generator was designed to generate trace concentrations of gases for gas sensing simulations. This feature makes it best suited for generating very low acetone concentrations, such as is obtainable in human breath. The concentrations of acetone vapor used in this study are 2.85 & 5.4ppm under 10%, 50% and 70% RH conditions respectively. To commence the experiment,

baseline resistance of the sensors at room RH (between 20% - 40%RH) was measured and recorded. Secondly, acetone vapor was delivered into the testing chamber housing the sensors. Inside the box, while the sensors interact with the in-flowing acetone vapor, the change in resistance due to this chemical interaction is measured simultaneously using the electrometer. The sensitivity of the sensor films to acetone at a given RH value, can be defined as the percentage change in resistance in the material due to acetone and is calculated, thus;

$$S\% = \left(\frac{R3 - R2}{R1}\right) \times 100$$

Where; S is sensitivity (%) to acetone, R1 is the baseline resistance (MΩ) under room RH, R2 is the resistance (MΩ) at a given RH condition without acetone in-flow and finally, R3 is the resistance (MΩ) at a given RH condition with acetone in-flow.

Acetone Sensor Device Design

The prototype of the sensor device as shown in Figure 2, is made up of 3 sub-units – the sensor, the signal acquisition & conditioning unit and the data visualization unit.

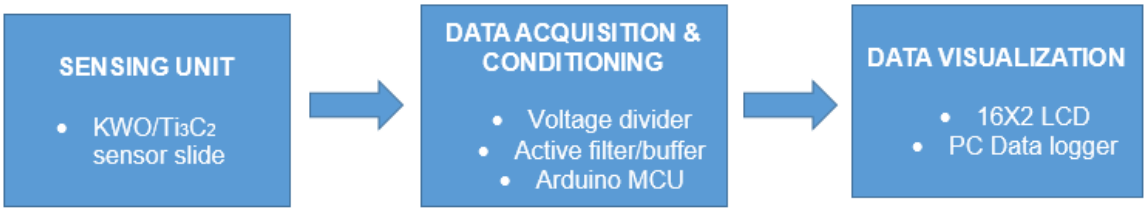

Figure 2: Showing the 3 functional units of the KWO/Ti_3C_2 prototype acetone sensor device.

The sensor unit is made up of the KWO/Ti_3C_2 sensor which interacts with trace concentration of acetone in a controlled environment. This unit also serves as an input to the signal conditioning unit of the device. For this chemiresistive sensor device, the signal acquisition & conditioning unit is designed based on a voltage divider principle; a known resistor and an unknown resistor connected in series (R_1 & R_2). Figure 3 shows a circuit diagram of the acetone sensor device. The KWO/Ti_3C_2 sensor is designated as the unknown resistor and an 18MΩ resister

as the reference or known resistor. The output signal of the voltage divider is connected to a low pass filter and a 9VDC powered µA741 Operational amplifier buffer, before being fed into the 8bit analog-to-digital converter (ADC) of the Arduino Nano microcontroller (A-MCU). The sensitivity to breath acetone is then computed by a custom program uploaded to the A-MCU. The DHT11 sensor is used to track the RH and temperature conditions.

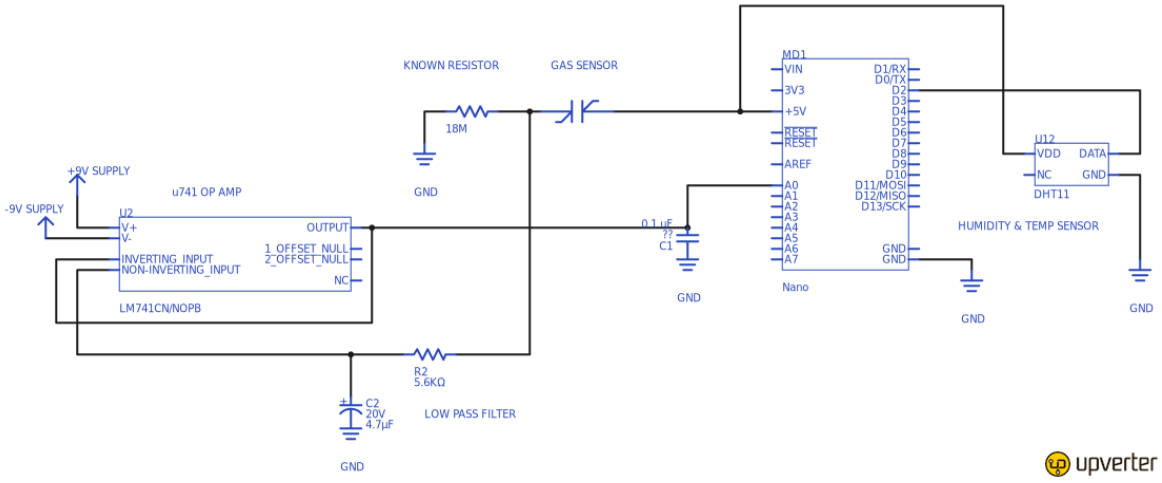

Figure 3: Schematic diagram of the KWO/Ti_3C_2 sensor device.

The data visualization unit is made up of a 16X2 LCD display and a real-time data logging platform, enabled by the Parallax microcontroller data acquisition add-on tool on Microsoft Excel. The data displayed in this unit include the sensitivity value (S%), humidity (RH%), temperature (T^oC), baseline resistance in air ($R_1M\Omega$), initial resistance at a given humidity value ($R_2M\Omega$) and final resistance due to exposure to 2.85ppm acetone ($R_3M\Omega$).

RESULTS AND DISCUSSION

Generally, performance of a chemiresistive sensor with regards to detection of an analyte gas largely depends on the chemical, electrical and structural properties. These properties influence the transfer of charges in the material and consequently, triggers a corresponding change in resistance(45,46). For a nanocomposite, such as the KWO/Ti_3C_2 sensor material, the response to acetone gas is a function of the collective properties of each constituent material and the composite. As previously reported, the KWO material has shown significant response to trace concentrations of acetone given its ferroelectric property(44).

Sensing Test

To investigate the prospects of an improved performance, which can be implicitly attributed to the novel combination of Ti_3C_2 and KWO nanomaterial films, control experiments were performed to compare performance of the individual Ti_3C_2 and KWO sensor films against their nanocomposite. The ratio of the elemental materials of the nanocomposite were varied in 3 samples.

As established, the high electrical conductivity of the Ti_3C_2 material is its strong selling point. However, the Ti_3C_2 material alone, did not yield any remarkable sensitivity to both 2.85ppm and 5.4ppm concentrations of acetone as shown in Figures 4 & 5. This suggests that, the Ti_3C_2 must have served as a charge sink to facilitate the ease of binding and unbinding of holes (majority carrier) in the KWO, due to Ti_3C_2's high electrical conductivity.

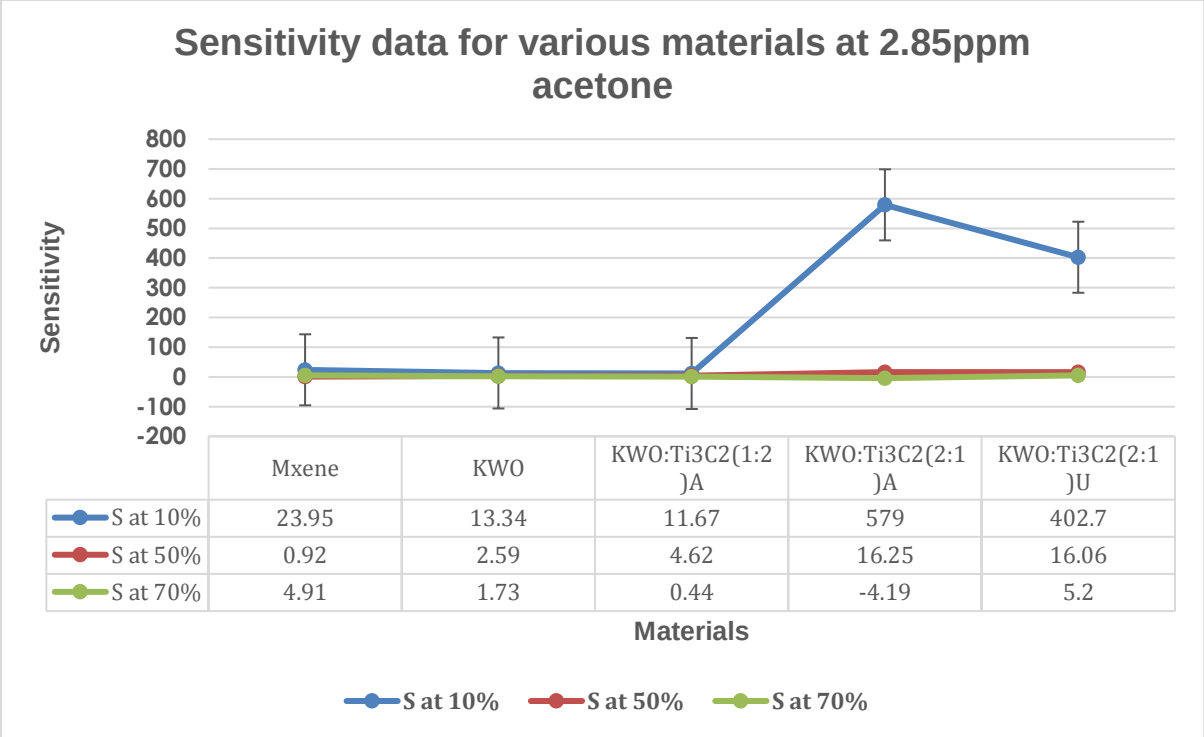

	Mxene	KWO	KWO:Ti3C2(1:2)A	KWO:Ti3C2(2:1)A	KWO:Ti3C2(2:1)U
S at 10%	23.95	13.34	11.67	579	402.7
S at 50%	0.92	2.59	4.62	16.25	16.06
S at 70%	4.91	1.73	0.44	-4.19	5.2

Figure 4: Sensitivity data for sensor films at 2.85ppm acetone. Ti_3C_2, KWO, annealed KWO/Ti_3C_2 (1:2), annealed KWO/Ti_3C_2 (2:1), and unannealed KWO/Ti_3C_2 (2:1).

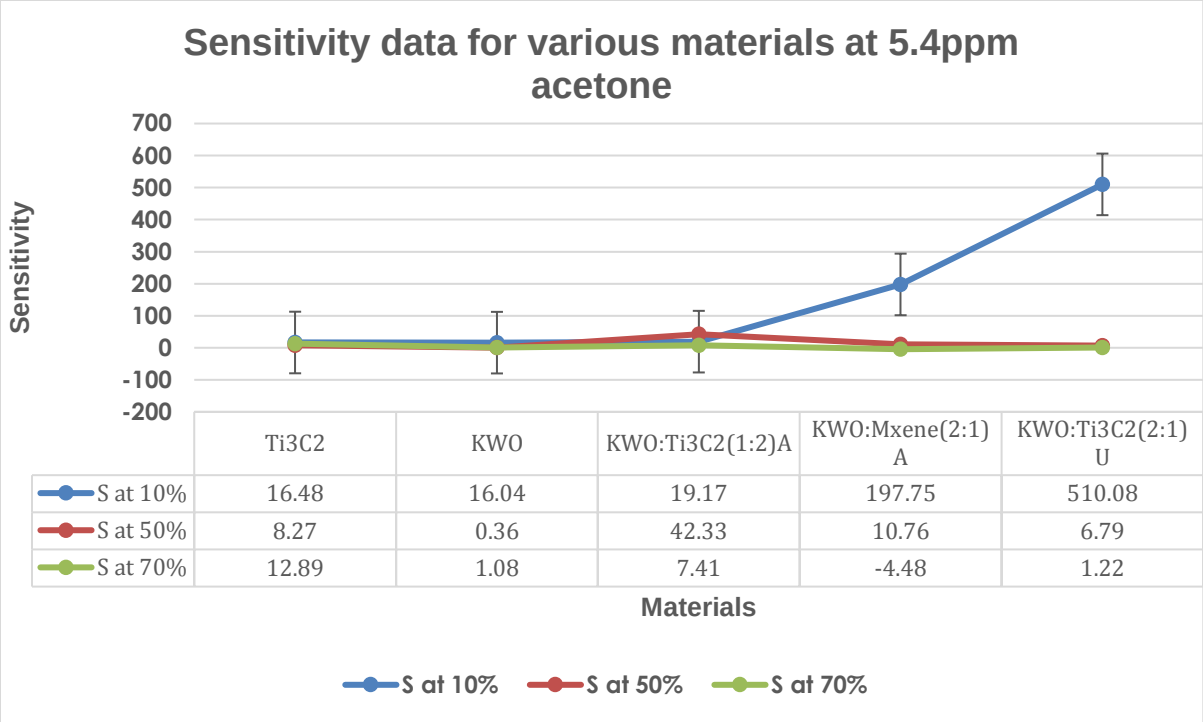

	Ti3C2	KWO	KWO:Ti3C2(1:2)A	KWO:Mxene(2:1)A	KWO:Ti3C2(2:1)U
S at 10%	16.48	16.04	19.17	197.75	510.08
S at 50%	8.27	0.36	42.33	10.76	6.79
S at 70%	12.89	1.08	7.41	-4.48	1.22

Figure 5: Sensitivity data for sensor films at 5.4ppm acetone. Ti_3C_2, KWO, annealed KWO/Ti_3C_2 (1:2), annealed KWO/Ti_3C_2 (2:1), and unannealed KWO/Ti_3C_2 (2:1).

The KWO film showed moderate sensitivity as shown in Figures 4 & 5 respectively. Such sensitivity has been attributed to the ferroelectric property and large surface area of KWO film, which fosters the sensitive interaction between KWO nanostructures and the high dipole moments of the acetone gas molecules(44).

However, the KWO/Ti_3C_2 films showed dramatic sensitivity to both concentrations of acetone. The annealed KWO/Ti_3C_2 (2:1) showed sensitivity of 579% and 402.7% to 2.85ppm and 5.4ppm acetone, respectively under 10% RH. Similarly, the unannealed KWO/Ti_3C_2 (2:1) sample showed sensitivity of 197.5% and 510.08% sensitivity to 2.85ppm and 5.4ppm concentration of acetone under 10% RH. The annealed KWO/Ti_3C_2 (1:2) showed no significant sensitivity in both concentrations.

Effect of Compositional Ratio

Based on the test results, it is safe to surmise that the most suitable compositional ratio for the KWO/Ti_3C_2 sensor in order to elicit a decent sensitivity to acetone, is the 2:1 ratio, regardless of the heat treatment method used during synthesis (annealed or unannealed). This implies that holes, as the major charge carriers in the p-type KWO semiconductor, remains the dominant player in the KWO/Ti_3C_2's mechanism of detection. Additionally, Md Rezuan in a recent study(44), revealed KWO's excellent performance in varying RH conditions. Accordingly, the response to high RH can be attributed to the Ti_3C_2 Mxene, which mainly stems from the interaction between the H_2O molecules and OH^- radicals on the functionalized surface Mxene(34). Righettoni et. al (22) reported a similar RH interference in an Si doped WO_3 breath acetone sensor, but this was resolved by increasing the operating temperature of the sensor. However, the latter method would be antithetical to the objective of developing a sensor with low power demands. Hence, increasing the ratio of the KWO to Ti_3C_2 in the nanocomposite, may overcome this limitation.

Effect of Ti_3C_2 Conductivity

Nevertheless, the role of the Ti_3C_2 cannot be over-looked. The high electrical conductivity of Ti_3C_2 Mxene is crucial in reducing the baseline resistance of the sensor to a decent level. The KWO sensor typically, displays a high resistance given the linear relationship between the resistance and the concentration of acetone; resistance increases as concentration of acetone increases. Due to this positive linearity, Wang et al in a related work, highlighted the limitation associated with very high resistance in the KWO sensor(28). Organic sensors with high impedance such as the KWO, introduce noise to any circuit and requires some improvement in the circuit to overcome this limitation. Conceivably, optimizing the sensing circuit to address this limitation, will also translate to an increase in the overhead cost of the sensor device. The addition

of Ti_3C_2 Mxene to KWO, decreased the baseline resistance of the KWO/Ti_3C_2 sensor, due to its high electrical conductivity. As a result, this does not only confer an economic cost advantage on the circuit, but an improved sensitivity due to the improved SNR as well.

Effect of Humidity

The sensitivity data showed significant response under 10% RH but no notable response at 50% and 70% RH. Expectedly, the resistance plot in Table 2 shows a corresponding low change in resistance from the initial resistance at room RH. In explaining this phenomenon, a cautious conjecture would be that, at lower humidity (≤10% RH), OH radicals on the Ti_3C_2 surface recombine with the holes (electron-hole recombination, EHR). This in-flow of electrons, results in the decrease of the majority carrier (holes), which consequently increases the resistance of the sensor. In higher RH conditions (50% - 70%), the H^+ from H_2O molecules react with the OH^- to form more H_2O molecules. The H_2O formation occurs at a much higher rate than the EHR, implying a lower change in resistance due to less reduction in the total number of majority carrier (holes). Hence, the low response at high humidity condition. Further investigation is required to improve the sensor response in high humidity.

Table 2: Resistance values in MΩ against different humidity values for the prototype sensor device.

R1@33.9%	RH	R_2(RH)	R_3 (acetone)
2.23	10%	3.79 MΩ	10.23 MΩ
2.23	50%	2.31MΩ	2.62 MΩ
2.23	70%	2.25 MΩ	2.34 MΩ

R1 is the resistance measured in air (room RH = 33.9%), R2 is the resistance at any given RH value (10%, 50% and 70%), R3 is the final resistance after exposure to 2.85ppm of acetone.

Sensor Device Performance

To investigate the performance of the prototype sensor device, the annealed KWO/Ti3C2 (ratio 2:1) film was used in the prototype device for the 2.85ppm acetone sensing test. Figure 6 shows results of the test at 10%, 50% and 70% RH conditions.

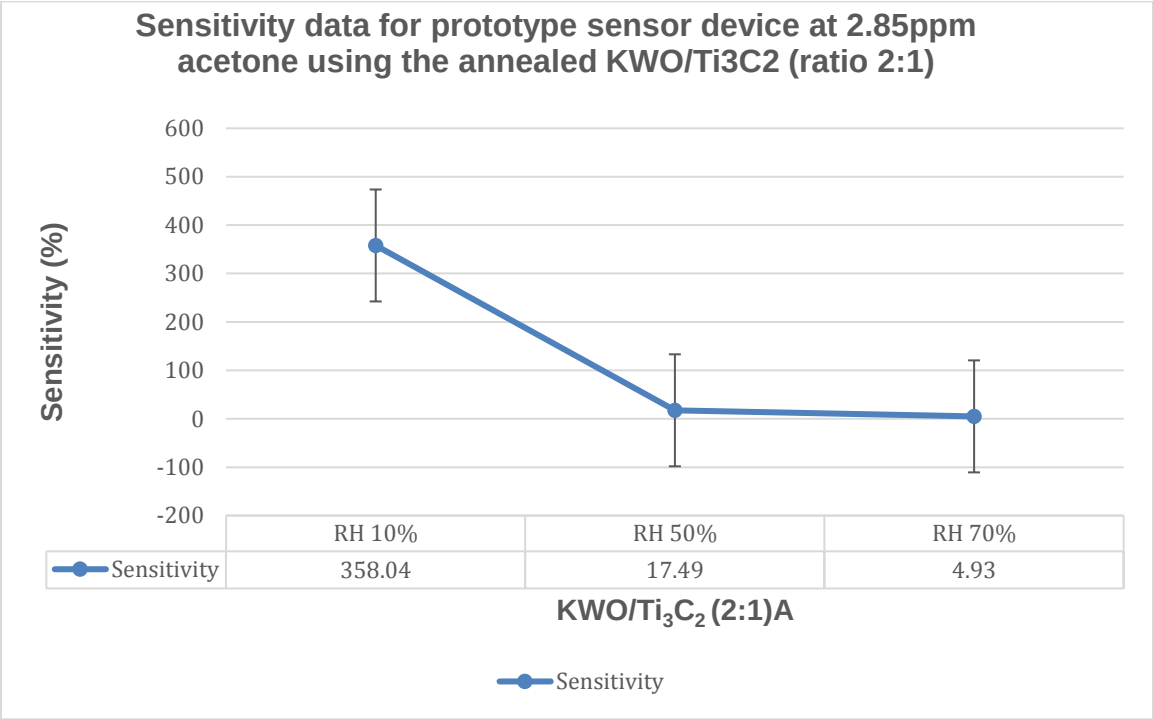

Figure 6: Sensitivity data for the acetone prototype device at 2.85ppm acetone. Experiments were done at 10%, 50% and 70% RH conditions.

The annealed KWO/Ti3C2 (2:1) sensor material coupled to the device, showed a significant sensitivity of 358.04% to 2.85ppm acetone, although this value is slightly lower than the 579% sensitivity recorded on the testing system setup. The sensitivity at 50%RH and 70%RH were 17.04% and 4.93% respectively and are consistent with the low sensitivity data reported in the testing setup for both RH conditions.

Since sensitivity of a chemiresistor is a function of the % change in resistance, this difference in sensitivity between the testing system and the device (579% and 358.04%) can be attributed to a limitation associated with the Arduino 8-bit ADC sampling rate. The higher 32-bit

sampling rate of the Keithley electrometer(47) used for resistance measurements in the testing system setup, allows for faster sampling of the constantly changing analog signal from nanocomposite film, as it interacts with acetone. Hence, the increased sensitivity values reported during the testing system tests. This limitation can be addressed using a MCU with a higher data sampling rate such as 32-bit, without compromising cost.

Effect of High Impedance Noise

In addition to the high SNR and high conductivity bestowed on this novel sensor by the Mxene compound, a first order active low pass filter was incorporated to further remove the high frequency noise from the power supply. The zero-output impedance of the 741 Op amp buffer in this active filter configuration, was used to eliminate the high impedance due to the nanocomposite film. This was also necessary as the Arduino has an analog input impedance of about 100MΩ and requires that any connection to its analog input, needs to be of a lower impedance. The Op amp serves this purpose. Additionally, the output signal or the input signal to the Arduino analog input was connected to a 0.1µF capacitor to steady the rapidly changing signal for the slower Arduino 8-bit ADC for sampling.

Device Size

The size of the final prototype device is approximately 10cm by 8cm in size and weighs about 1kg. These dimensions meet the specifications for an ideal portable device for breath acetone measurement. Figure 7 compares the sizes of different acetone sensing systems with the KWO/Ti_3C_2 device, being very portable.

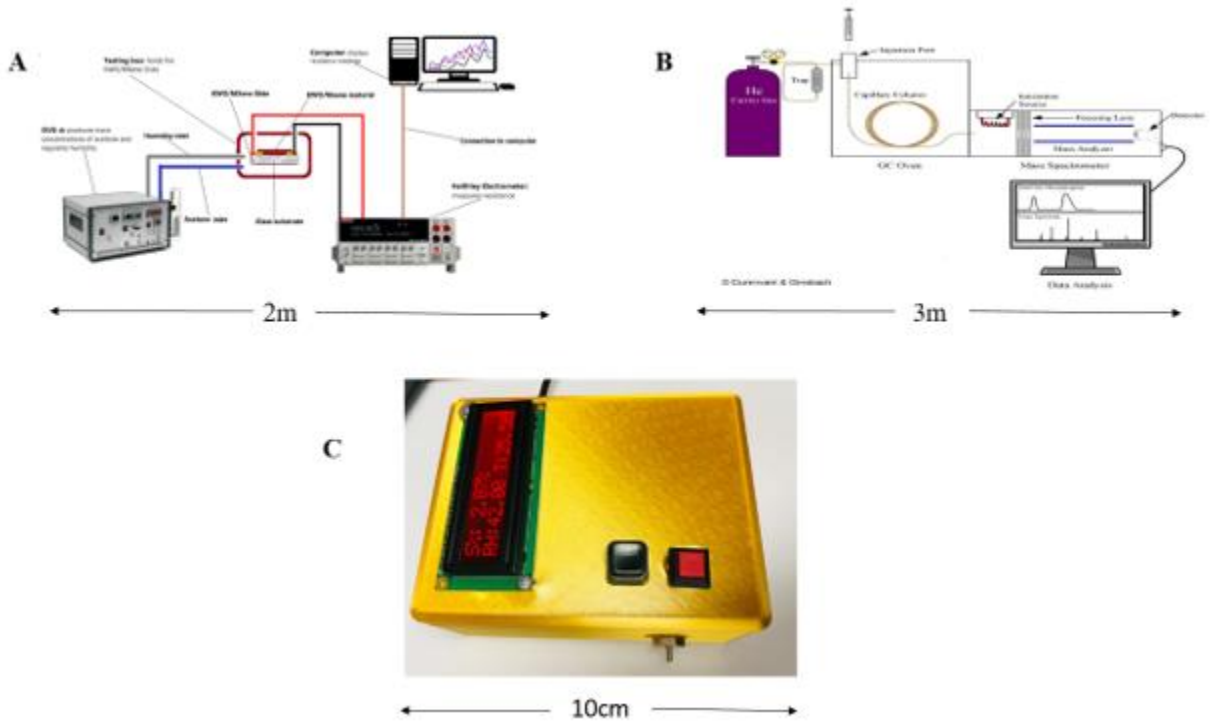

Figure 7: Approximate dimension in length of 3 different acetone testing systems. A). Experimental testing system comprising of the OVG, an electrometer, sensor box and a PC, with an approximate length of 2 meters. B). GC/MS testing system with an approximate length of 3m (Image courtesy of (48)) and C). The novel KWO/Ti_3C_2 prototype acetone sensing device with a length of 10cm.

FUTURE WORK

The prototype sensor device has been designed and functions according to the desired specifications for an ideal breath acetone monitor. However, to fully achieve the purpose of this glucose measurement, further work is required to establish a correlation between the sensitivity, acetone concentration and blood glucose levels using a machine learning or statistical approach. This would entail mapping of sensitivity values from different breath samples to the blood glucose concentration of the respective patients.

Secondly, advanced fabrication techniques can be employed to further scale down the size of the device to a microscale and to control the noise effect due to high impedance, an example is the use of a PCB guard ring technique to shield aspects of the circuits from interference.

Thirdly, the device needs to be optimized to sensitively detect acetone at higher RH levels. Other options for reducing the effect of RH include the introduction of anhydrous compounds such as $CaSO_4$(49).

CONCLUSION

The importance of a simple, yet accurate testing technique for blood glucose in diabetics has been discussed and current measurement techniques reviewed. Metallic oxide semiconductors have so far proven to be the useful in achieving this objective, but limitations of operating temperature and sensitivity still exist. Results reported in this study, have shown that the KWO/Ti_3C_2 sensor sensitively detects acetone at a concentration of 2.85ppm and as well as operate at room temperature with a high SNR due to the high electrical conductivity of the Ti3C2 Mxene. However, further work is necessary to extend the sensor performance to higher humidity conditions given the human breath is about 90% RH.

REFERENCES

1. International Diabetes Federation. IDF DIABETES ATLAS [Internet]. 9th ed. Suvi Karuranga, editor. International Diabetes Federation; 2019 [cited 2020 Mar 25] p. 4. Available from: https://www.idf.org/e-library/welcome/copyright-permission.html
2. Bruen D, Delaney C, Florea L, Diamond D. Glucose sensing for diabetes monitoring: recent developments. Sensors (Basel). 2017 Aug 12;17(8).
3. Clement S, Braithwaite SS, Magee MF, Ahmann A, Smith EP, Schafer RG, et al. Management of diabetes and hyperglycemia in hospitals. Diabetes Care. 2004 Feb;27(2):553–591.
4. American Diabetes Association. Diagnosis and classification of diabetes mellitus. Diabetes Care. 2014 Jan;37 Suppl 1:S81–90.
5. Kawasaki E. Type 1 diabetes and autoimmunity. Clin Pediatr Endocrinol. 2014 Oct;23(4):99–105.
6. Ozen G, Zanfardino A, Confetto S, Piscopo A, Casaburo F, Tinto N, et al. The Association of Autoimmune Diseases with Type 1 Diabetes Mellitus in Children Depends Also by the Length of Partial Clinical Remission Phase (Honeymoon). Int J Endocrinol. 2020 Jan 4;2020:2630827.
7. Atkinson M. Thirty Years of Investigating the Autoimmune Basis for Type 1 Diabetes.
8. Taylor R. Insulin resistance and type 2 diabetes. Diabetes. 2012 Apr;61(4):778–779.
9. Noctor E, Dunne FP. Type 2 diabetes after gestational diabetes: The influence of changing diagnostic criteria. World J Diabetes. 2015 Mar 15;6(2):234–244.
10. Rydosz A. A negative correlation between blood glucose and acetone measured in healthy and type 1 diabetes mellitus patient breath. J Diabetes Sci Technol. 2015 Jul;9(4):881–884.
11. De Ruyter ML, Harrison BA. Hyperglycemia and diabetic ketoacidosis. Complications in Anesthesia. 2007;
12. Ruzsányi V, Kalapos MP. Breath acetone as a potential marker in clinical practice. J Breath Res. 2017 Jun 1;
13. Güntner AT, Kompalla JF, Landis H, Theodore SJ, Geidl B, Sievi NA, et al. Guiding Ketogenic Diet with Breath Acetone Sensors. Sensors (Basel). 2018 Oct 28;18(11).
14. Lehnert AS, Behrendt T, Ruecker A. Performance of SIFT-MS and PTR-MS in the measurement of volatile organic compounds at different humidities. Atmospheric …. 2019;
15. Moser B, Bodrogi F, Eibl G, Lechner M, Rieder J, Lirk P. Mass spectrometric profile of exhaled breath--field study by PTR-MS. Respir Physiol Neurobiol. 2005 Feb 15;145(2-3):295–300.
16. Sun MX GZ. A Ringdown Breath Acetone Analyzer: Performance and Validation Using Gas Chromatography-Mass Spectrometry. J Anal Bioanal Tech. 2014;S7(012).
17. Review_Conducting Polymers as Chemiresistive Gas Sensing Materials_A Review.pdf.
18. Nasiri N, Clarke C. Nanostructured chemiresistive gas sensors for medical applications. Sensors (Basel). 2019 Jan 23;19(3).
19. Jiang Y, Tang N, Zhou C, Han Z, Qu H, Duan X. A chemiresistive sensor array from conductive polymer nanowires fabricated by nanoscale soft lithography. Nanoscale. 2018 Nov 15;10(44):20578–20586.
20. Usman F, Dennis JO, Ahmed AY, Meriaudeau F, Ayodele OB, Rabih AAS. A Review of Biosensors for Non-Invasive Diabetes Monitoring and Screening in Human Exhaled Breath. IEEE Access. 2019;7:5963–5974.

21. Fine GF, Cavanagh LM, Afonja A, Binions R. Metal oxide semi-conductor gas sensors in environmental monitoring. Sensors (Basel). 2010 Jun 1;10(6):5469–5502.
22. Righettoni M, Tricoli A, Pratsinis SE. Si:WO(3) Sensors for highly selective detection of acetone for easy diagnosis of diabetes by breath analysis. Anal Chem. 2010 May 1;82(9):3581–3587.
23. Qiu Z, Hua Z, Li Y, Wang M, Huang D, Tian C, et al. Acetone Sensing Properties and Mechanism of Rh-Loaded WO3 Nanosheets. Front Chem. 2018 Sep 11;6:385.
24. Maziarz W, Kusior A, Trenczek-Zajac A. Nanostructured TiO2-based gas sensors with enhanced sensitivity to reducing gases. Beilstein J Nanotechnol. 2016 Nov 15;7:1718–1726.
25. Kumar S, Pavelyev V, Mishra P, Tripathi N. A review on chemiresistive gas sensors based on carbon nanotubes: Device and technology transformation. Sensors and Actuators A: Physical. 2018 Nov;283:174–186.
26. Tomer VK, Singh K, Kaur H, Shorie M, Sabherwal P. Rapid acetone detection using indium loaded WO3/SnO2 nanohybrid sensor. Sensors and Actuators B: Chemical. 2017 Dec;253:703–713.
27. Wang D, Zhang Q, Hossain MR. High Sensitive Breath Sensor Based on Nanostructured K2W7O22 for Detection of Type 1 Diabetes. IEEE Sensors …. 2018;
28. Hossain MR, Zhang Q, Johnson M, Wang D. Highly Sensitive Room-Temperature Sensor Based on Nanostructured K_2W_7O22 for Application in the Non-Invasive Diagnosis of Diabetes. Sensors (Basel). 2018 Oct 31;18(11).
29. Johnson ME, Zhang Q, Wang AD. Kxwo is a novel ferroelectric nanomaterial for application as a room temperature acetone sensor. Nanomaterials (Basel). 2020 Jan 28;10(2).
30. Huang K, Li Z, Lin J, Han G, Huang P. Two-dimensional transition metal carbides and nitrides (MXenes) for biomedical applications. Chem Soc Rev. 2018 Jul 17;47(14):5109–5124.
31. Shahzad F, Alhabeb M, Hatter CB, Anasori B, Man Hong S, Koo CM, et al. Electromagnetic interference shielding with 2D transition metal carbides (MXenes). Science. 2016 Sep 9;353(6304):1137–1140.
32. Alhabeb M, Maleski K, Anasori B, Lelyukh P, Clark L, Sin S, et al. Guidelines for Synthesis and Processing of Two-Dimensional Titanium Carbide ($Ti_3 C_2$ MXene). Chem Mater. 2017 Sep 26;29(18):7633–7644.
33. Peng Y-Y, Akuzum B, Kurra N, Zhao M-Q, Alhabeb M, Anasori B, et al. All-MXene (2D titanium carbide) solid-state microsupercapacitors for on-chip energy storage. Energy Environ Sci. 2016;9(9):2847–2854.
34. Yurish S. Advances in Sensors: Reviews, Vol. 7: Physical and Chemical Sensors: Design, Applications & Networks.
35. Xing R, Xu L, Song J, Zhou C, Li Q, Liu D, et al. Preparation and gas sensing properties of in2o3/au nanorods for detection of volatile organic compounds in exhaled breath. Sci Rep. 2015 Jun 1;5:10717.
36. Jamalabadi H, Alizadeh N. Enhanced Low-Temperature Response of PPy-WO_3 Hybrid Nanocomposite Based Gas Sensor Deposited by Electrospinning Method For Selective and Sensitive Acetone Detection. IEEE Sens J. 2017 Apr 15;17(8):2322–2328.
37. Das S, Ghosh S, Kumar R, Bag A, Biswas D. Highly Sensitive Acetone Sensor Based on Pd/AlGaN/GaN Resistive Device Grown by Plasma-Assisted Molecular Beam Epitaxy. IEEE Trans Electron Devices. 2017 Nov;64(11):4650–4656.

38. Xu H, Gao J, Li M, Zhao Y, Zhang M, Zhao T, et al. Mesoporous WO3 Nanofibers With Crystalline Framework for High-Performance Acetone Sensing. Front Chem. 2019 Apr 18;7:266.
39. Gong J, Li Y, Chai X, Hu Z, Deng Y. UV-Light-Activated ZnO Fibers for Organic Gas Sensing at Room Temperature. J Phys Chem C. 2010 Jan 21;114(2):1293–1298.
40. Al-Hardan NH, Abdullah MJ, Abdul Aziz A, Ahmad H, Low LY. ZnO thin films for VOC sensing applications. Vacuum. 2010 Jul;85(1):101–106.
41. Wang X, Qin H, Pei J, Chen Y, Li L, Xie J, et al. Sensing performances to low concentration acetone for palladium doped LaFeO3 sensors. Journal of Rare Earths. 2016 Jul;34(7):704–710.
42. Teleki A, Pratsinis SE, Kalyanasundaram K, Gouma PI. Sensing of organic vapors by flame-made TiO2 nanoparticles. Sensors and Actuators B: Chemical. 2006 Dec;119(2):683–690.
43. Kim SJ, Koh H-J, Ren CE, Kwon O, Maleski K, Cho S-Y, et al. Metallic Ti3C2Tx MXene Gas Sensors with Ultrahigh Signal-to-Noise Ratio. ACS Nano. 2018 Feb 27;12(2):986–993.
44. Hossain MR, Ama O, Zhang Q. Investigation of Different Materials as Acetone Sensors for Application in Type-1 Diabetes Diagnosis. … Journal of Scientific …. 2019;
45. Ji H, Zeng W, Li Y. Gas sensing mechanisms of metal oxide semiconductors: a focus review. Nanoscale. 2019 Dec 21;11(47):22664–22684.
46. Jaaniso R, Tan OK. Semiconductor gas sensors. books.google.com; 2013.
47. Keithley Instruments, Inc. Model 2000 Multimeter. 2010 Aug;
48. Dunnivant F, Ginsbach J. Flame atomic absorbance and emission spectroscopy and inductively coupled spectrometry-mass spectrometry. Whitman College. 2009;
49. Hossain MR. Highly Sensitive Room Temperature Sensor Based on Nanostructured K2W7O22 for Diagnosis Diabetes. 2019;